# The Dragset copper–zinc deposit: a deformed, volcanogenic sulphide occurrence in the Løkken greenstones, Central Norway

KENNETH GEORGE McQUEEN

McQueen, K. G.: The Dragset copper–zinc deposit: a deformed, volcanogenic sulphide occurrence in the Løkken greenstones, Central Norway. *Norsk Geologisk Tidsskrift*. Vol. 70, pp. 1–19. Oslo 1990. ISSN 0029–196X.

Brittle-ductile deformation of a primary, volcanogenic sulphide deposit at Dragset has produced a stack of folded and faulted massive sulphide layers now underlying a flattened and elongated stringer ore zone. The orebody was overturned, deformed and metamorphosed under mid-greenschist facies conditions during at least two major phases of deformation. The host rocks are mostly massive, sheet-flow and pillowed greenstones which retain the geochemical signature of tholeiitic ocean-floor basalts. Metabasalts in the stringer zone show ore-related hydrothermal alteration marked by enrichment in Fe and MgO, and depletion in CaO and $Na_2O$. Ore types include: massive, fine-grained pyritic and siliceous ores with minor Cu and Zn; chalcopyrite- and sphalerite-rich pyritic ores; and chalcopyrite-pyrrhotite stringer ores. Primary ore fabrics are only preserved on a macroscale and include compositional layering in sphalerite-rich ores, and possibly some replacement and relict fragmentary textures. Textures in massive pyritic ores mostly reflect cataclastic flow and recrystallization during early isoclinal folding and axial plane shearing of the ore layers. This style of deformation is probably typical for massive pyritic ores subjected to high shear stress under low grade metamorphic conditions (350–450°C).

*K. G. McQueen, School of Applied Science, Canberra College of Advanced Education, P.O. Box 1 Belconnen, A.C.T., 2616 Australia.*

The Dragset copper–zinc deposit is a small, greenstone-hosted, pyritic sulphide deposit located 8.5 km west of Løkken Verk in the western Trondheim district of central Norway (Fig. 1). The deposit was probably discovered before 1700 and worked intermittently until 1909 (Borchgrevink 1954). Incomplete production records combined with estimates of remaining ore and the size of the mullock dumps suggest a premining resource of about 100,000 tonnes of ore grading 2% Cu, 2.5% Zn and 20 g/t Ag.

Dragset is one of a number of stratabound, massive sulphide deposits known in the Løkken area. Other occurrences include the major Løkken deposit (25 million tonnes), the Høidal deposit (ca. 100,000 tonnes) and numerous very minor deposits (e.g. Fjellslette, Åsskjerp, Holum, Åmot, Kong Karl). All of these deposits are of similar type, but with differences in detail and scale. Most occur in a regionally inverted sequence of dominantly metabasic rocks, referred to as the Løkken greenstones. The Løkken deposit was the largest known copper–zinc deposit in Norway; however, after more than 300 years of exploitation most of the ore has been removed and mining operations at Løkken and in the surrounding area have now ceased.

There are several descriptions of the Løkken and Høidal deposits, including a petrological and geochemical study of the host greenstones near Løkken (Carstens 1951; Vokes 1960; Grenne et al. 1980; Grenne 1986). The study reported here was aimed at extending this work and expanding the knowledge of deposit types and ore-forming processes in the Løkken area. The Dragset deposit lies in a more deformed part of the sequence than that enclosing the Løkken or Høidal deposits, and it was thought that a detailed structural analysis of the ore environment might give a better appreciation of the style and mechanisms of ore deformation in the region. Although small, the deposit makes an excellent case study due to its good three-dimensional exposure revealed in outcrop, several small open pits, connecting underground workings and drill core.

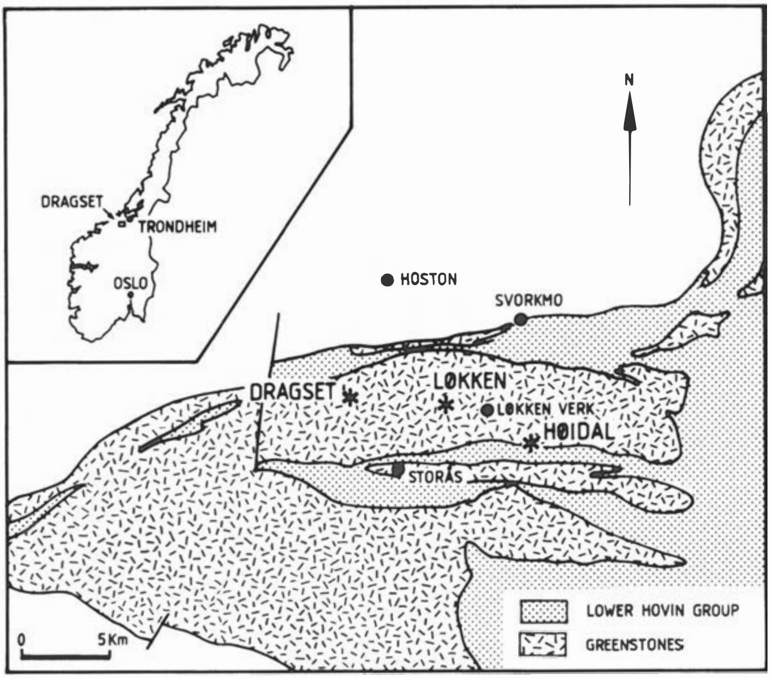


*Fig. 1.* Location and geological setting of the Dragset deposit in central Norway. Also shown are the locations of the Løkken and Høidal deposits.

# General geology

The Løkken greenstones consist dominantly of metabasic volcanic rocks and associated metadolerites and metagabbros with intercalated jasper and sulphidic chert beds (vasskis). These rocks have been correlated with the Støren Group to the east and are stratigraphically overlain by the Lower Hovin Group, within the Caledonian Trondheim Nappe complex (e.g. Wolff 1976). The greenstones are probably Cambrian to Early Ordovician in age (Ryan et al. 1980; Grenne, 1988).

In the Dragset area the greenstone succession can be subdivided into two major sequences (Fig. 2). In the mine area and further east there are pillowed metabasalts, hyaloclastitic and pillow breccias, thin layers of reworked hyaloclastite and small intrusive bodies of altered gabbro, dolerite and plagioclase porphyrite. This sequence is devoid of siliceous or pelagic metasediments and vasskis layers. Pillow morphologies in the less deformed lavas indicate that the sequence is upside down. Stratigraphically above (structurally below) this sequence and outcropping mainly to the west and south of Dragset is a sequence of pillowed and massive metabasalts with numerous intercalated jasper and vasskis layers, some conglomeratic units and minor felsic metavolcanics. Altered dolerite dykes cut the metabasalts but coarser grained metagabbros have not been observed. Pillowed metabasalts generally show close-packed pillows and much less interpillow hyaloclastite material than in the lower sequence. The two sequences are well defined by aeromagnetic data, with magnetite-bearing vasskis units in the stratigraphically higher sequence giving prominent magnetic anomalies.

The two distinct greenstone sequences at Dragset appear to correlate with two subgroups of upper and lower metavolcanites recognized on lithological and geochemical criteria in the Løkken–Høidal area (Grenne et al. 1980).

# Regional metamorphism and structure

The Løkken greenstones have undergone low grade regional metamorphism and show varying degrees of deformation. In the Dragset area, metamorphic mineral assemblages are consistent with a mid-greenschist facies grade of metamorphism. Absence of prehnite–pumpellyite and pumpellyite–chlorite–quartz bearing assemblages in mafic rocks suggests peak temperatures above 350°C for pressures of 2–4 kb (Winkler 1979).

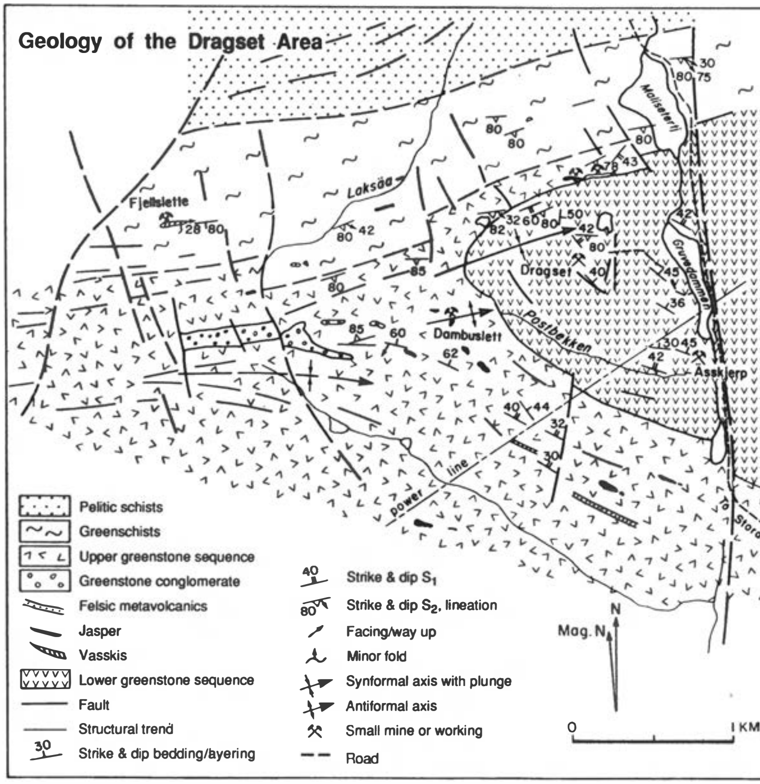


*Fig. 2.* Detailed geological map of the Dragset area.

Stability of muscovite–chlorite–quartz and absence of staurolite, cordierite and aluminous silicates in pelitic schists indicates a maximum temperature less than 500°C. The typical assemblage of albite–actinolite–chlorite–epidote–sphene in metabasalts, and particularly the presence of albite rather than oligoclase, together with the presence of stilpnomelane and chloritoid in some greenstones and biotite and chlorite in others, suggest metamorphic temperatures between 350° and 450°C (Winkler 1979). It has not been possible to determine the confining pressure; however, this was probably less than 4 kb, given the tectonic setting and structural position of the Støren Group within the Trondheim Nappe Complex.

The major structural feature of the Løkken region is the approximately east–west trending Løkken synform. The Dragset deposit occurs near the western closure of this structure, close to the main axis (Fig. 2). In this area the synform plunges 35° ENE, but further east, near Løkken, the axis has a more gentle westerly plunge. Observations at Dragset and in the surrounding area indicate that the synform is asymmetric with a steep, south-dipping and strongly deformed northern limb, and a moderate, north-dipping southern limb. South of the major synform the Løkken greenstones and Lower Hovin Group rocks appear to be folded into a series of tight antiforms and synforms, while on the northern side these rocks are thrust-faulted against older and higher grade metamorphic, allochthonous rocks of the Gula Group (Wolff 1976).

In the Dragset area, folding associated with formation of the Løkken synform (here designated $F_2$) affected an earlier tectonic surface ($S_1$) as well as the primary stratigraphic layering ($S_0$). An axial plane surface ($S_2$) was heterogeneously developed during this $F_2$ folding. In the southern and central parts of the area $S_2$ is generally seen as a weakly developed, widely spaced cleavage, but towards the north it becomes progressively more penetrative and in the tight northern limb of the synform is a well-developed schistosity. Pillow structures in metabasalts show a parallel increase in strain (Fig. 3).

The earlier $S_1$ surface also shows a heterogeneous imprint throughout the area and is generally subparallel to original layering (Fig. 8). At

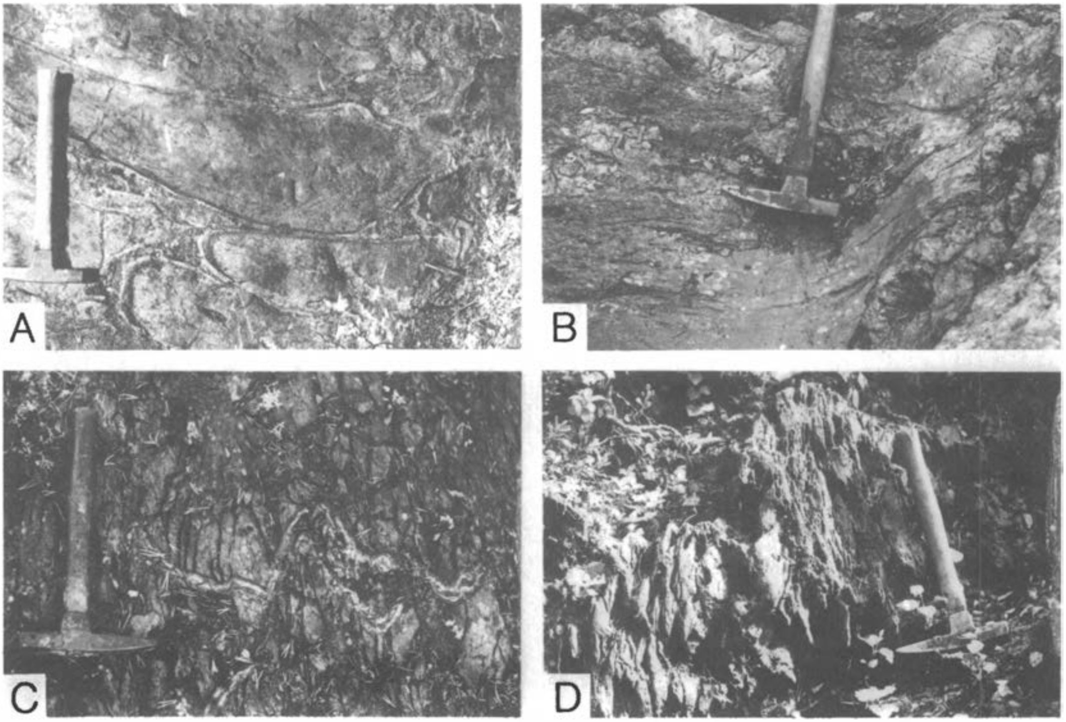


*Fig. 3.* Photographs of pillowed metabasalts from south to north across the Dragset area showing progressive increase in strain: (A) weakly deformed pillow basalts from near the Dragset mine showing inverted facing; (B) glaciated surface showing small flattened pillows and foliated inter-pillow material; (C) strongly deformed pillow structures showing development of intra-pillow foliation as well as folding and transposition of pillow rims; (D) greenschist containing small pillow rim fragments.

its strongest development, $S_1$ is a penetrative cleavage or fracture surface but in less deformed rocks it is defined by weak fractures, flattening of pillows and amygdales and elongation of clasts in fragmentary rocks. Lack of well-defined marker units and limited exposure make it difficult to interpret this surface. However, observations of deformed massive ore layers in the Dragset deposit suggest that $S_1$ is related to an early stage of large-scale recumbent folding (designated $F_1$). Where ore layers have been affected by recumbent $F_1$ folds, $S_1$ is developed as an axial surface to these folds and is folded by small, open $F_2$ folds. Low-strength and multi-layered parts of the greenstone stratigraphy (including the ore sequence) appear to have preferentially accommodated strain during the $F_1$ folding.

Several lineations are developed in the deformed rocks including a common $S_1$–$S_2$ intersection lineation ($L_2$, Fig. 8). In some areas where the greenstones contain bedded tuffaceous or sedimentary units, an aggregate streaking lineation is developed in $S_1$ and is apparent where this surface is parallel to $S_2$. On the northern limb of the Løkken synform the $S_2$ schistosity commonly shows a crenulation lineation and minor kink folding, presumably related to deformation subsequent to $F_2$ folding. The crenulation shows a variable pitch, generally between 25° and 50° to the east.

Faulting of the greenstones has produced: (1) large low-angle thrust faults; (2) major steeply dipping faults; and (3) numerous smaller faults and fractures. Major low-angle thrusts have sliced up the sequence east of the Dragset area (e.g. west of the Orkla River and above the Løkken orebody, Grenne et al. 1980) but only small-scale thrusts have been seen near Dragset. The steep faults show mainly vertical displacements and generally trend approximately N–S, although in the centre of the synform east of Løkken Verk, some form ENE and WNW trending conjugates. A major N–S fault east of Dragset, along Gruvedammen valley, clearly offsets the stratigraphy and aeromagnetic trends on both limbs of the Løkken synform. Calculations based on the limb offsets and respective dips indicate approximately 500 m of downthrow on the eastern side. Smaller faults and fractures show various orientations but are commonly developed normal to the limbs of the Løkken synform and also subparallel to the axial surface of this structure (Fig. 2).

## Nature of the Dragset deposit

### *Host rocks*

The Dragset deposit occurs within the stratigraphically lower greenstone sequence (Fig. 2). The immediate host rocks are massive to variably foliated and fractured, fine-grained metabasalts which mainly occur in sheet flows (1–6 m thick), with some pillowed layers and interflow, hyaloclastitic and pillow breccia zones. Altered dolerite dykes cut the metabasalts and some have also intruded the orebody. The structural hangingwall to the deposit (stratigraphic footwall) contains more abundant pillowed zones and hyaloclastitic breccias. Plagioclase porphyrites have also been observed in drill core. The rocks structurally below the ore zone are mainly massive sheet-flow metabasalts showing a blocky, polygonal jointing, but 80 m below the ore (higher in the stratigraphy) there is a prominent zone of pillowed metabasalts cut by metadolerite dykes. Pillow morphologies in this unit clearly indicate that the mine sequence is inverted and hence that the orebody is upside down (Fig. 3A). Unlike the nearby Løkken and Høidal deposits there are no jasper or vasskis layers associated with the ores.

*Table 1.* Major and trace element compositions of host greenstones at Dragset.

| | Structural footwall | | | Structural hangingwall | | | Stringer Zone | | | | Meta-dolerite | Meta-gabbro |
|---|---|---|---|---|---|---|---|---|---|---|---|---|
| wt% | D-14 | D-13 | D2-17 | D3-9 | D-22 | D-19 | D-16 | D-18 | D1-3 | D1-2 | D1-1 | D-15 |
| $SiO_2$ | 43.81 | 48.54 | 49.73 | 51.42 | 48.18 | 49.71 | 46.70 | 47.79 | 30.45 | 27.51 | 51.36 | 46.52 |
| $TiO_2$ | 2.03 | 1.30 | 1.19 | 1.31 | 1.29 | 1.22 | 1.64 | 1.35 | 1.49 | 1.81 | 0.87 | 1.64 |
| $Al_2O_3$ | 14.37 | 14.37 | 12.76 | 14.42 | 13.76 | 14.15 | 13.90 | 13.48 | 14.37 | 18.23 | 14.29 | 14.04 |
| $Fe_2O_3$ | 2.79 | 3.68 | 1.78 | 1.81 | 2.77 | 2.46 | 2.90 | 4.96 | 3.33 | 4.47 | 2.46 | 2.67 |
| FeO | 9.07 | 7.24 | 7.95 | 9.49 | 7.57 | 7.57 | 8.37 | 4.76 | 22.91 | 19.17 | 6.24 | 8.27 |
| MnO | 0.21 | 0.19 | 0.20 | 0.19 | 0.17 | 0.22 | 0.20 | 0.20 | 0.22 | 0.24 | 0.15 | 0.19 |
| MgO | 7.33 | 6.95 | 7.95 | 6.50 | 7.68 | 7.36 | 8.29 | 9.62 | 9.36 | 16.59 | 8.93 | 7.50 |
| CaO | 9.58 | 8.80 | 8.28 | 4.43 | 9.98 | 9.00 | 8.97 | 6.70 | 2.33 | 1.47 | 8.72 | 9.26 |
| $Na_2O$ | 3.9 | 4.2 | 4.4 | 5.6 | 3.5 | 4.5 | 3.3 | 3.9 | 1.9 | 0.1 | 4.2 | 4.2 |
| $K_2O$ | 0.08 | 0.06 | 0.05 | 0.05 | 0.06 | 0.07 | 0.05 | 0.02 | 0.02 | 0.38 | 0.04 | 0.11 |
| $P_2O_5$ | 0.17 | 0.10 | 0.09 | 0.10 | 0.08 | 0.09 | 0.12 | 0.09 | 0.08 | 0.12 | 0.04 | 0.13 |
| $H_2O^+$ | 4.05 | 2.74 | 3.21 | 3.33 | 2.76 | 2.99 | 3.52 | 5.11 | 9.63 | 10.66 | 3.10 | 3.35 |
| $H_2O^-$ | 0.20 | 0.13 | 0.09 | 0.09 | 0.18 | 0.11 | 0.13 | 0.12 | 0.09 | 0.25 | 0.11 | 0.20 |
| $CO_2$ | 2.34 | 0.22 | 1.66 | 0.54 | 0.24 | 0.92 | 0.18 | 0.22 | 0.15 | 0.16 | 0.56 | 0.64 |
| S | 0.19 | 0.16 | 0.04 | 0.16 | 0.05 | 0.06 | 0.01 | 2.86 | 6.32 | 0.44 | 0.02 | 0.09 |
| O≈S | 0.05 | 0.04 | 0.01 | 0.04 | 0.01 | 0.02 | – | 1.41 | 2.85 | 0.21 | – | 0.02 |
| Total | 100.07 | 98.64 | 99.37 | 99.40 | 98.24 | 100.41 | 98.28 | 99.77 | 99.80 | 101.39 | 101.09 | 98.80 |
| ppm | | | | | | | | | | | | |
| V | 383 | 312 | 281 | 412 | 302 | 297 | 328 | 316 | 368 | 548 | 244 | 298 |
| Cr | 93 | 222 | 131 | 26 | 255 | 170 | 324 | 314 | 414 | 488 | 442 | 139 |
| Ni | 52 | 64 | 51 | 22 | 65 | 58 | 79 | 56 | 33 | 71 | 109 | 50 |
| Co | 45 | 51 | 45 | 35 | 52 | 45 | 52 | 34 | 88 | 85 | 45 | 56 |
| Cu | 66 | 43 | 67 | 42 | 48 | 54 | 27 | 93 | 1.22% | 13 | 56 | 101 |
| Zn | 101 | 99 | 150 | 165 | 85 | 84 | 240 | 306 | 588 | 129 | 69 | 86 |
| Pb | <10 | <10 | <10 | 10 | 27 | 16 | <10 | 34 | 10 | 17 | <10 | <10 |
| Sr | 113 | 59 | 144 | 34 | 115 | 96 | 241 | 40 | 69 | <5 | 136 | 160 |
| Y | 44 | 24 | 25 | 24 | 28 | 24 | 32 | 25 | 26 | 34 | 22 | 31 |
| Zr | 149 | 90 | 81 | 89 | 80 | 79 | 107 | 90 | 91 | 104 | 52 | 112 |
| Ba | 30 | 26 | 41 | 19 | <10 | 19 | 10 | <10 | 15 | 84 | 15 | 30 |

In all samples Rb, Nb <5 ppm; La, Ce <10 ppm.

Chemical analyses are by XRF except $H_2O$, $CO_2$, S (gravimetrically); $Na_2O$ (flame photometry); FeO (titration). Analyst NGU, Trondheim.

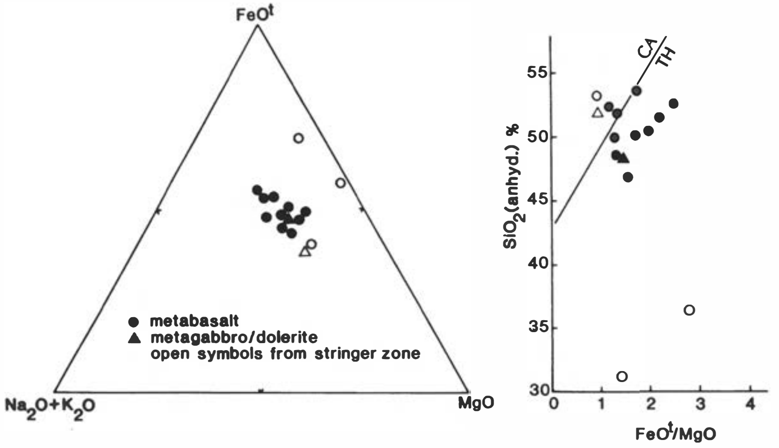


*Fig. 4.* Major element plots for host greenstones at Dragset. CA is calcalkaline field and TH tholeiitic field, FeO$^t$ is total Fe as FeO.

In thin section, the host greenstones generally appear deformed and metamorphically recrystallized with few relict igneous textures, at least near the deposit. The rocks commonly consist of decussate and fascicular amphibole, anhedral to subhedral albite ($<An_5$) granular epidote, small dispersed aggregates of sphene and irregular patches of chlorite. Some rocks close to the massive ores contain biotite in the groundmass. Epidote, calcite and quartz also form secondary veins. The chlorite in the metabasalts is generally pycnochlorite or ripidolite with about equal proportions of Fe and Mg. Chloritic rocks close to the deposit contain a more magnesium chlorite (>23% MgO). Amphiboles in the greenstones generally have actinolitic compositions with up to 1 Al and 0.5 Na atoms per formula unit. Some chloritic rocks associated with the stringer ores contain tremolite with very low Al and Na contents.

Microscopic observation of tectonite fabrics in the host rocks reveals that the $S_1$ foliation is defined by aligned aggregates of sphene, epidote and in some cases chlorite. This surface probably formed during or just after the regional metamorphism. At the mine, the $S_2$ surface is defined by micro-fractures, calcite–quartz veins and some chlorite veins which transect the main metamorphic fabric. Where $S_2$ is a penetrative schistosity (e.g. north of the Dragset deposit), the rocks show preferred orientation of chlorite and sphene aggregates, break-up and realignment of amphibole prisms parallel to the schistosity, and rotation of epidote porphyroblasts within this surface. These textures attest to the post-metamorphic timing of $S_2$ and the $F_2$ folding.

## *Host rock geochemistry*

Major and trace element analyses of greenstones from the stratigraphic footwall and hangingwall to the Dragset deposit suggest original tholeiitic basalt compositions (Table 1, Fig. 4). There is some uncertainty attached to the major element trends due to the altered nature of the rocks; however, discriminant diagrams based on typically immobile elements generally confirm this parentage and further suggest that the greenstones at Dragset, and from the Løkken area in general, originally had ocean-floor affinities (Fig. 5; Pearce & Cann 1973; Pearce 1975; Grenne et al. 1980). Apparent depletion of Cr in some samples may indicate mobility of this element during very strong alteration or, less likely, extreme magmatic fractionation processes (cf. Grenne et al. 1980).

## *The ores*

In its present form the Dragset deposit consists of a series of thin (<3 m) massive sulphide layers which show major fracturing, shearing and folding (Figs. 6, 9). These layers are mostly conformable with the $S_1$ surface in the enclosing greenstones (and probably also with the primary layering) and have been folded with this surface during subsequent ($F_2$) folding. Contacts between the layers and enclosing greenstones vary from sharp, possibly tectonized surfaces, to irregular and partly gradational boundaries. To the northeast of the massive ores, in the stratigraphic footwall, there is a clearly defined stringer zone containing pervasive veinlet and disseminated sulphides (Figs. 6, 7).

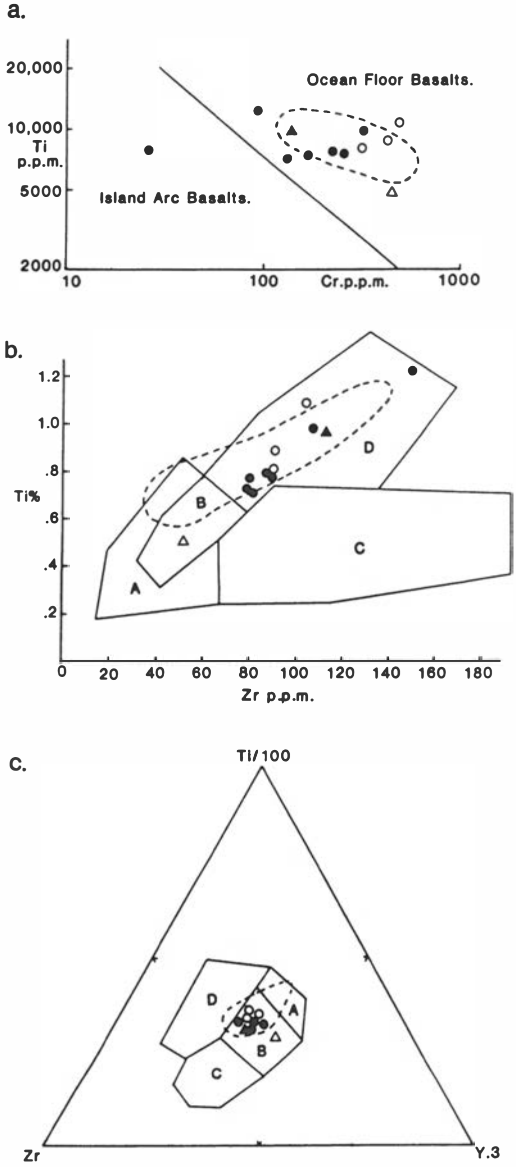


*Fig. 5.* Trace element discriminant diagrams for host greenstones at Dragset (symbols as in Fig. 4) and greenstones from the Løkken area (dashed field, Grenne et al. 1980). In (b) ocean floor basalts plot in fields B and D, low-K tholeiites in fields A and B, and calcalkaline basalts in fields C and B (Pearce & Cann 1973). In (c) low-K tholeiites plot in fields B and C, and within plate basalts in field D.

*Ore structures and geometry.* – Two groups of folds are preserved in the massive ores: early isoclinal, recumbent folds of the ore layers and contained banding; and upright, open to tight folds of ore layers and the $S_1$ host rock foliation (Figs. 8, 9). Recumbent folds are generally well defined only where the ore layers are thin. More commonly the massive pyritic ore has broken up in the hinge zones of these folds, resulting in segmented or separated massive ore limbs. Shear movements parallel to the axial surfaces of the recumbent folds have also caused some imbrication of the massive ore layers. Where fold hinges are still preserved they mostly plunge at about 30° ESE (Fig. 8). It is generally not possible to determine facing in these folds, but at the extreme northwest end of the deposit, stringer zone rocks, which are stratigraphically lower in the sequence, have been folded around a segmented massive ore hinge indicating facing to the south (Fig. 9A). The upright folds are common on a mesoscale in the remnants of ore left in the old mine workings. These folds are almost coaxial with the recumbent ($F_1$) folds (Fig. 8) but are clearly later structures as they fold the axial surface to the recumbent folds. Some of the massive ore layers show thickening in the hinge zones of these upright folds.

As well as affecting the form of the massive ores, folding has largely determined the present orientation of the orebody, such that the massive ore layers now lie parallel to the regional $S_1$ foliation. The ore zone as a whole is elongated parallel to the $F_1$ (and $F_2$) fold plunge direction.

The massive ores are cut by a number of steeply dipping faults showing two predominant strike directions (ca. E–W and NNE–SSW, Fig. 8). Movement has been mostly vertical with a strike slip component in some cases. Block faulting about three major fault zones has produced significant offsets of the northeast dipping massive ore layers (Fig. 6). In the southwest part of the deposit massive ores have also been rotated within a wide fault zone.

The stringer ores appear to represent an original footwall feeder to the massive sulphides, which now occupies the structural hangingwall due to overturning of the deposit. Some rocks in this zone are strongly foliated (pencil schists) with pronounced development of both the NE dipping $S_1$ and steeply dipping $S_2$ surfaces. This enhanced foliation development is probably due to the higher chlorite content of the altered rocks, particularly in areas close to the massive ores. The broad zone of pyrite veining and dissemination which encloses the main stringer ore is now extended parallel to the $F_1$ fold plunge direction and information from drill core suggests that the stringer zone dips gently northeast and has been

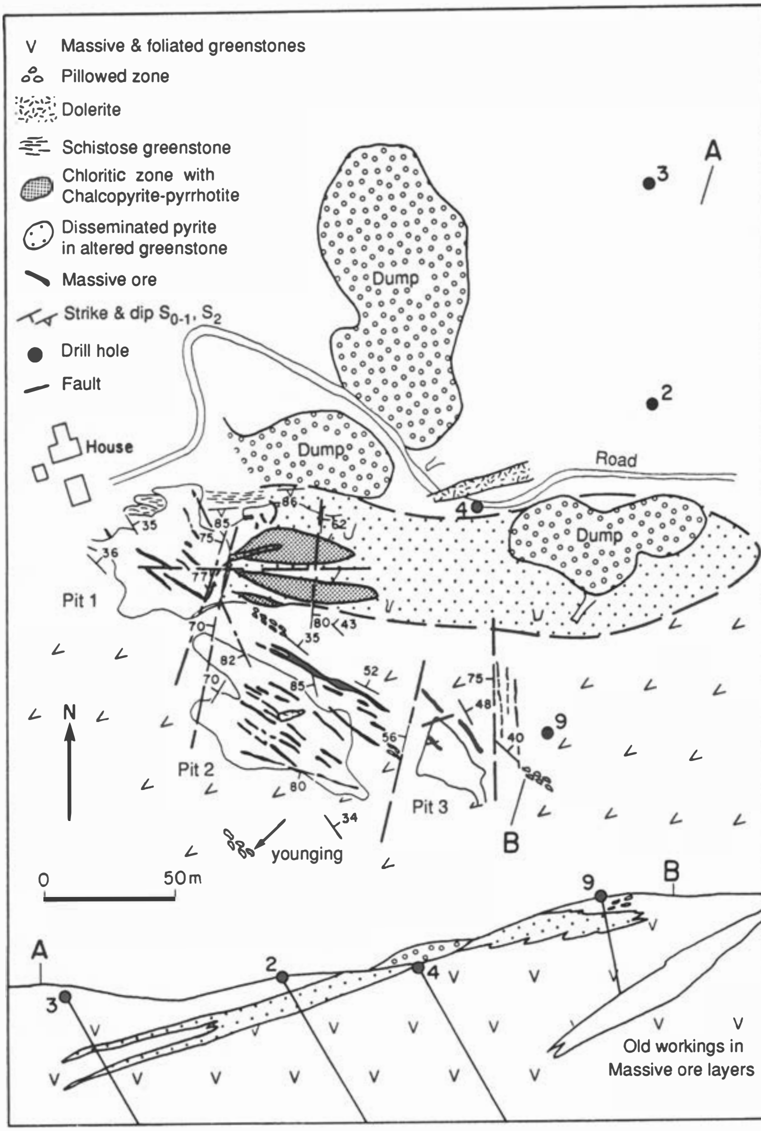


*Fig. 6.* Detailed geological plan and section of the Dragset deposit. Positions of massive ore layers are projected to Level 2 in the mine and based on the location of unmined remnants combined with data from old mine plans.

flattened in the $S_1$ direction (Fig. 6). Its intersection with the massive ore zone plunges approximately 20°NNW and most of the zone was probably higher up dip and is now eroded away.

*Ore types and fabrics.* – There are two major ore types at Dragset: Disseminated-veinlet sulphides in the stringer zone; and massive pyritic ores. There is also a variety of ore subtypes. The stringer zone contains irregular masses of highly chloritic, veinlet ore with abundant chalcopyrite–pyrrhotite and lesser pyrite, as well as surrounding areas of fine disseminated pyrite and pervasive pyrite veining containing only traces of base metal sulphides. Massive ore subtypes include: fine-grained pyritic ore with minor chalcopyrite and sphalerite; highly siliceous and coarser-grained pyritic ore developed near the stringer zone; and chalcopyrite- and sphalerite-rich pyritic ores, some showing banding.

Irregular banding in massive ores is generally defined by sphalerite-rich layers a few mm to several cm wide. In some cases the banding is subparallel to the margins of the ore layers but in other areas it may be folded or very irregular. Chalcopyrite-rich zones and patches can be seen

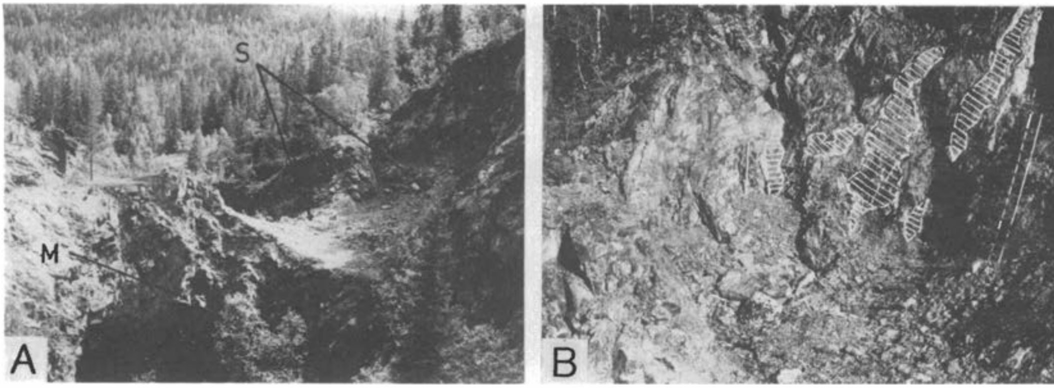


*Fig. 7.* A. View northeast across Pit 1 at the Dragset deposit, showing the location of stringer ore (S) and massive ore lenses (M). B. Detailed view of exposed area of stringer ore zone. White shaded areas are pods of chloritic material containing chalcopyrite–pyrrhotite rich veinlets.

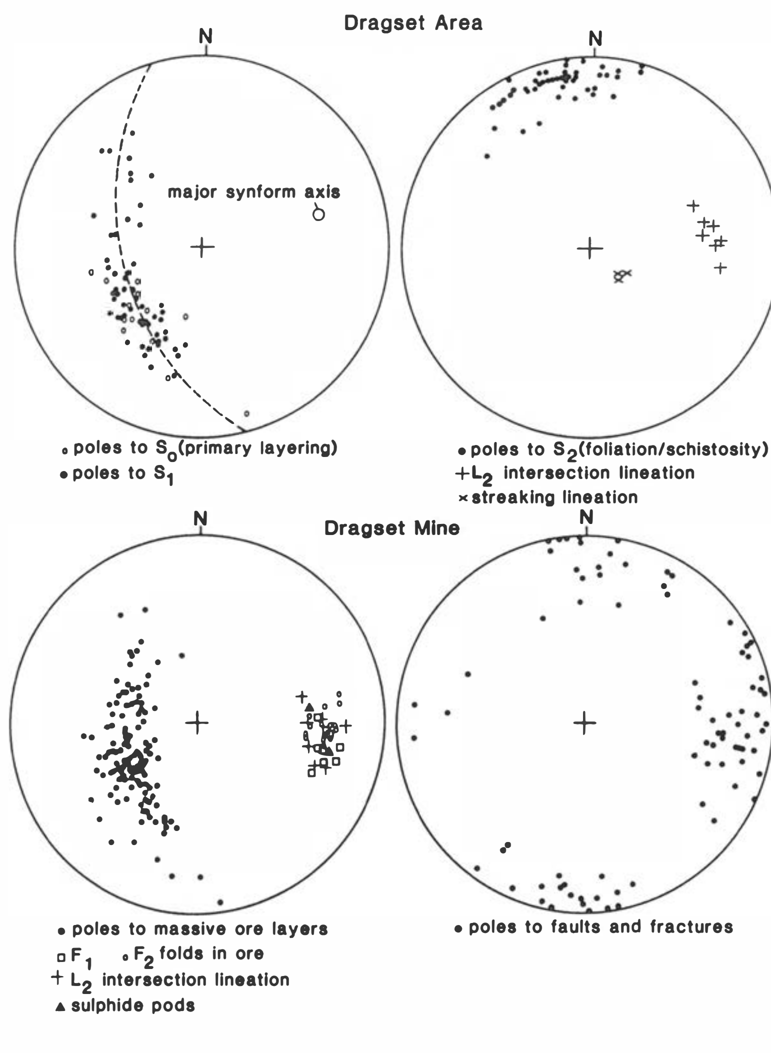


*Fig. 8.* Equal area stereo plots of structural elements in the greenstone sequence in the Dragset area and at the Dragset deposit.

in the Cu-rich massive sulphides. Small veins of remobilized chalcopyrite are common around the massive ores and also cut interlayered greenstone bands. The pyrite-rich massive ores commonly show a fragmentary fabric with brecciated, irregular and angular fragments or blocks of fine-grained pyrite, veined by coarser-grained and recrystallized pyrite. Chalcopyrite is also commonly concentrated in these veins. The veins are 1–5 mm wide and clearly formed later than the fine-grained pyrite.

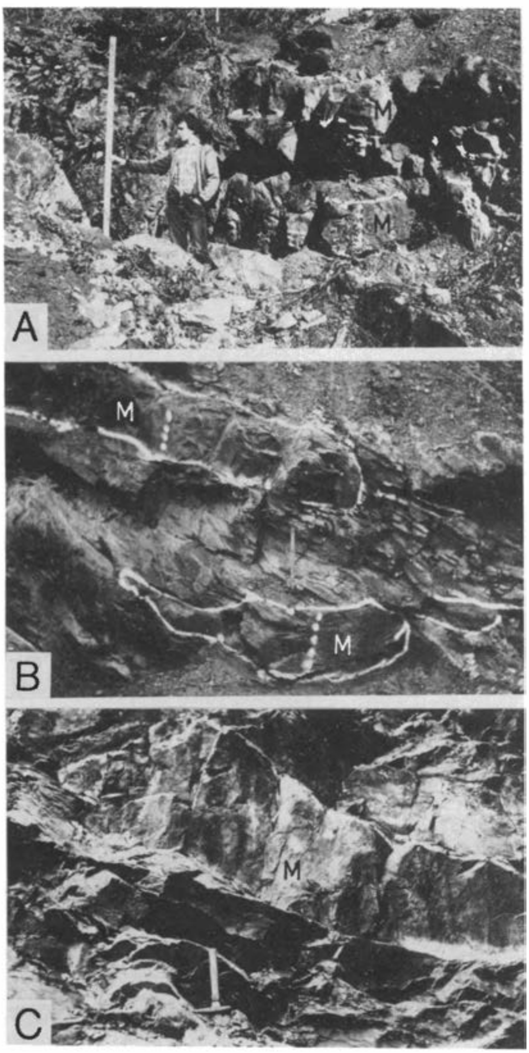


*Fig. 9.* Mesoscopic ore structures at Dragset. A. Disrupted $F_1$ fold of massive ore layer (M). The fold hinge is on the right and facing is to the left of the photograph. B. Massive ore layer (M) showing recumbent isoclinal $F_1$ folding, hinge disruption and break-up of limbs by faulting. C. Segmented and thickened massive ore layer (M) overlying foliated greenstones showing $F_2$ folding of the $S_1$ surface.

At the microscale, three types of ore textures can be recognized. These include replacement-type textures (mostly primary), relict deformation textures, particularly in pyrite, and textures related to grain growth and recrystallization. Massive pyritic ores generally consist of aggregates of fine-grained (0.02–0.6 mm) subhedral pyrite with intergranular, anhedral chalcopyrite, minor sphalerite, silicates (including quartz, chlorite, plagioclase and stilpnomelane) and trace pyrrhotite. Larger pyrite grains and aggregates commonly show 'chalcopyrite-healed' microfractures and are typically enclosed or rimmed by finer-grained, granulated pyrite. In pyrite-rich samples granulated aggregates of pyrite define a foliation. Some ores contain larger recrystallized pyrite subhedra (up to 3 mm), particularly where the pyrite has developed in a dominant chalcopyrite matrix. Pyritic ores close to late-stage faults preserve evidence of cataclastic deformation including extreme granulation of the pyrite and preferred orientation of elongate grains and aggregates parallel to numerous trans-aggregate fractures (Fig. 10D). Some caries-type textures in pyrite, particularly against sphalerite, may be primary replacement textures; however, most small-scale primary textures appear to have been modified or destroyed by deformation and recrystallization. There is no evidence of fine-grained colloform textures like those seen in the less deformed Høidal deposit (cf. Grenne & Vokes 1986).

In the massive ores, pyrite occurs in several distinct forms, possibly representing different stages of growth or recrystallization. These include large subhedra with numerous small (<0.03 mm) inclusions of chalcopyrite, sphalerite, pyrrhotite and gangue minerals. Most of these inclusions were probably incorporated during recrystallization growth of the pyrite. However, the tiny pyrrhotite inclusions may reflect small-scale compositional readjustments due to slight loss of sulphur and increase in FeS activity during deformation and metamorphic recrystallization of the pyrite. Other pyrite types observed are inclusion-free, fine-grained pyrite showing symplectite-like intergrowth with chalcopyrite; and porous pyrite developed as rims around earlier pyrite subhedra. The latter is probably a supergene pyrite. Copper-rich massive ores consist of subhedral pyrite grains dispersed through a fine-grained chalcopyrite matrix (Fig. 10A).

Sphalerite occurs in low-Zn ores as a minor

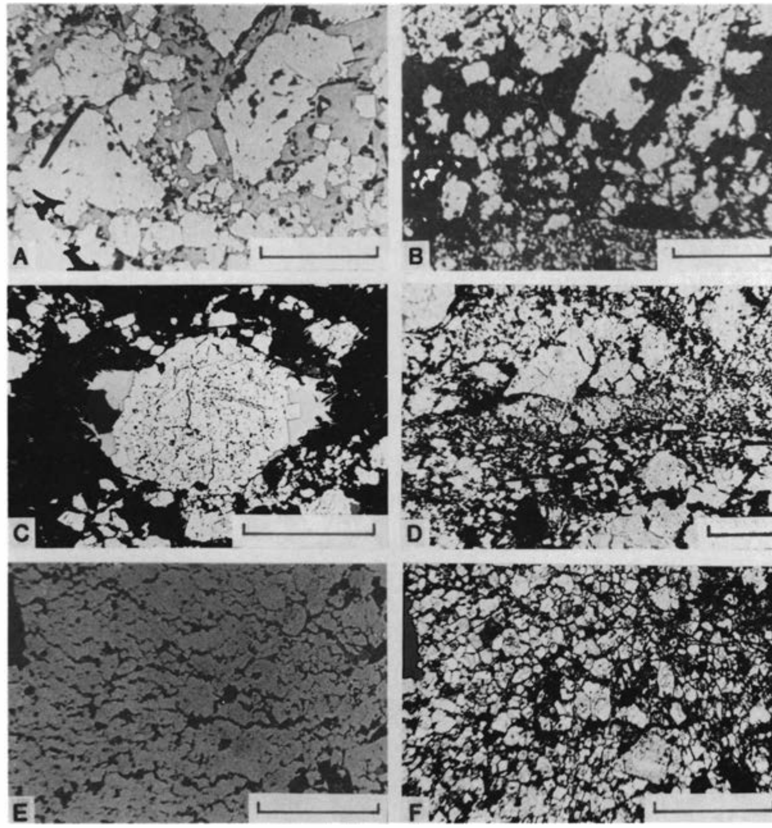


*Fig. 10.* Photomicrographs of some ore textures at the Dragset deposit. A. Chalcopyrite-rich massive ore with chalcopyrite matrix enclosing subhedral pyrite grains. Gangue is mostly stilpnomelane. Sample 8719. B. Sphalerite-rich band in massive pyritic ore showing partial replacement of pyrite (lighter) by sphalerite (darker). Sample 8777. C. Pyrite aggregate, showing pressure shadows of chalcopyrite and sphalerite, enclosed in a foliated, chloritic groundmass. Sample 8788. D. Pyritic ore from a late-stage fault zone showing typical cataclastic fabric. Sample 8788. E. Massive pyritic ore showing preferred orientation of granulated pyrite aggregates. This probably represents a recrystallized cataclastic fabric. Sample 8805. F. Same field of view as (E) after etching with nitric acid. This has revealed the recrystallized, euhedral nature of pyrite grains within the fabric. Sample 8805. All photographs taken in plane polarized reflected light. Scale bars are 0.4 mm.

phase in small anhedral aggregates with chalcopyrite, and as small inclusions in pyrite. Some of the inclusions show chalcopyrite disease; however, the sphalerite occurring intergranular to pyrite is free of this. In Zn-rich banded ores additional sphalerite occurs in separate zones that pervade the pyritic host. Pyrite inclusions and grains at the margins of these bands are highly irregular and embayed, suggesting partial replacement by sphalerite (Fig. 10B). The sphalerite-rich zones also commonly contain abundant, subhedral grains of magnetite (0.02–0.5 mm), some with rimming aggregates of pyrrhotite, as well as small blebs of minor chalcopyrite. Presence of magnetite may reflect a higher oxygen fugacity during sphalerite deposition or possibly later reaction of oxidized Zn-bearing fluids with early deposited pyrite to form sphalerite and magnetite. Sphalerite from throughout the deposit generally has a moderate Fe content (13–17 mole % FeS, from 24 microprobe analyses) with the lowest Fe in Zn-rich ores.

Monoclinic pyrrhotite is a common trace constituent in the massive ores and in some comprises up to 5% of the sulphides. In addition to forming small inclusions in pyrite, pyrrhotite occurs as larger, irregular aggregates, mostly associated with chalcopyrite in Cu-rich ores. It also occurs in cross-cutting aggregates along fractures, suggesting some later pyrrhotite introduction or remobilization. Some of the pyrrhotite shows secondary, probably supergene, alteration to mackinawite.

Stringer ores close to the massive ore layers consist of irregular veins of intergrown chalcopyrite and pyrrhotite in a chlorite-albite rich gangue. The chalcopyrite contains minor, subhedral and partly embayed pyrite grains (<1 mm) and small anhedral or star-shaped inclusions of sphalerite. Minute (<12 μm) grains of telluride minerals (including altaite, tellurobismuth and rucklidgeite) also occur within these sulphides.

No Ag-rich minerals were detected in the massive ores, suggesting that minor Ag is hosted either by the common sulphides themselves (cf. Harris et al. 1984) or in undetected, submicroscopic inclusions of Ag minerals.

*Ore geochemistry.* – Ore compositions were determined for 22 chip channel samples of massive and stringer ores (Table 2 and Fig. 11). The ores are clearly Fe-rich, reflecting their predominantly pyritic nature. There is a surprisingly wide variation in Cu/Zn ratios throughout the orebody, ranging from 0.08 to 19.4 (mean 0.81) for the massive ores. The Ag content ranges from 4 to 41 ppm and there is no apparent correlation between Ag and any of the other elements. Lead values are extremely low (<250 ppm) and Pb also shows no obvious correlation with the other elements. The Co content of the ore varies between 20 and 700 ppm while Ni values are low (<110 ppm) and fairly constant. Cadmium shows strong positive correlation with Zn, suggesting that it is mainly hosted by sphalerite.

Major disruption of the thin massive ores at Dragset by folding and faulting makes it difficult to detect systematic metal variations or zoning in the deposit. It is virtually impossible to reconstruct the massive ores and determine the relative positions of the now separate ore lenses; however, the following gross features are apparent. Sulphides in the stringer zone and in massive ores located close to this structure are relatively Cu- and Fe-rich (Fig. 11). Some of the massive sulphides appear to be enriched in Zn at the expense of Fe, and samples showing relatively higher Zn

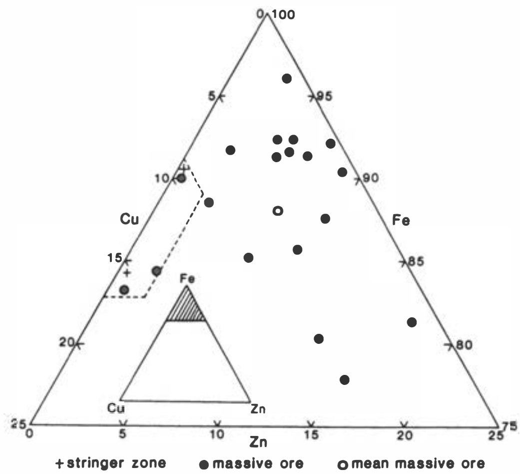


*Fig. 11.* Dragset ore compositions plotted in terms of Fe–Cu–Zn. Enclosed area includes stringer ores and siliceous massive ores directly above the stringer zone.

*Table 2.* Mean compositions and ranges for massive ores from the Løkken and Høidal deposits and massive and disseminated ores from Dragset.

| | Løkken | | Høidal | Dragset | |
|---|---|---|---|---|---|
| wt% | 1 | 2 | 3 | 4 | 5 |
| Fe | – | 38.0 | – | 36.3 (18.0–34.5) | 18.7 |
| Cu | 2.15 | 2.3 | 1.71 (0.01–10.20) | 2.20 (0.17–6.32) | 2.79 |
| Zn | 2.35 | 1.8 | 7.11 (0.01–29.10) | 2.73 (0.14–7.31) | 0.06 |
| S | – | 42.0 | – | 39.0 (21.2–48.8) | 7.5 |
| p.p.m. | | | | | |
| Ag | 18 | 6 | 36 (2–115) | 19 (4–44) | 10 |
| Cd | 70 | 100 | 208 (3–960) | 92 (8–242) | 5 |
| Co | 448 | 800 | 247 (16–1910) | 212 | 141 |
| Ni | 35 | 10 | 37 (11–106) | 51 (40–80) | 83 |
| Mn | 185 | 700 | 121 (17–340) | 171 (62–535) | 1382 |
| Pb | 334 | 200 | 837 (32–4070) | 99 (30–235) | 14 |
| Cu/Zn | 0.91 | 1.28 | 0.24 | 0.81 | 46.5 |
| Zn/Cd | 336 | 180 | 342 | 297 | 116 |
| n | | | 62 | 19 | 2 |

– = not analysed. Analyses (except No. 2) by A.A.S. following digestion in $HNO_3$ and HCl and in fuming $HNO_3$ for Ag. Fe determined as total Fe by titrimetric analysis. S determined gravimetrically. n = number of samples.

1. Continuous mill head sample for Løkken massive ore for 1982 (Astrup section). Tor Grenne (unpubl. data).
2. Typical analysis of massive ore from Løkken (Wallenberg section). Data from Vokes (1960).
3. Mean composition and range for massive ores from Høidal. Tor Grenne (1986).
4. Mean composition and range for massive ores from Dragset. Data from this study.
5. Mean composition of two disseminated stringer zone ore samples from Dragset. Data from this study.

generally come from areas more distal from the stringer zone, either along strike, or up the folded stack of massive ore layers. This pattern is consistent with the metal zoning observed in some other volcanogenic Cu–Zn deposits (e.g. Sangster 1972) and probably due to precipitation of sphalerite from hydrothermal solution in cooler and more distal parts of the ore-forming system (Large 1977; Solomon & Walshe 1979).

## *Hydrothermal alteration*

In ore deposits from metamorphic terrains it can be difficult to distinguish ore-related hydrothermal alteration from the effects of regional metamorphism and early-stage ocean-floor metamorphism. In many cases the alteration mineralogies are similar, particularly for low grade metamorphism. Criteria for recognizing these different effects include evidence for regionally pervasive metamorphic alteration, as distinct from more intense local alteration associated with the deposit, and geochemical evidence for major element gains and losses which are generally more pronounced with hydrothermal alteration because of the open nature of the system.

At Dragset it is clear that there has been considerable hydrothermal alteration around the stringer zone. This is indicated by the extensive chloritization, pyritization and lesser silicification around this zone, as well as gross chemical changes apparent in some of the major element plots (Fig. 4). This is confirmed by ratio variation diagrams which compare major elements as a ratio over an element considered to have been immobile during alteration (Pearce 1968; Nicholls 1988). In this case Ti has been taken as the constant divisor, as good correlation with other likely immobile elements, such as Zr and Cr, suggests that Ti has been relatively immobile. Under the alteration conditions pertaining at Dragset most Ti was probably incorporated and effectively immobilized in sphene, a mineral which remained stable throughout the dynamothermal metamorphism. The scattered patterns on some of the variation diagrams (Fig. 12) suggest changes to CaO, MgO and possibly $SiO_2$ contents in most of the greenstones during pervasive metamorphism and ocean-floor alteration. However, comparisons between normal host rocks and metabasalts from around the stringer zone indicate marked enrichment in Fe and MgO, and

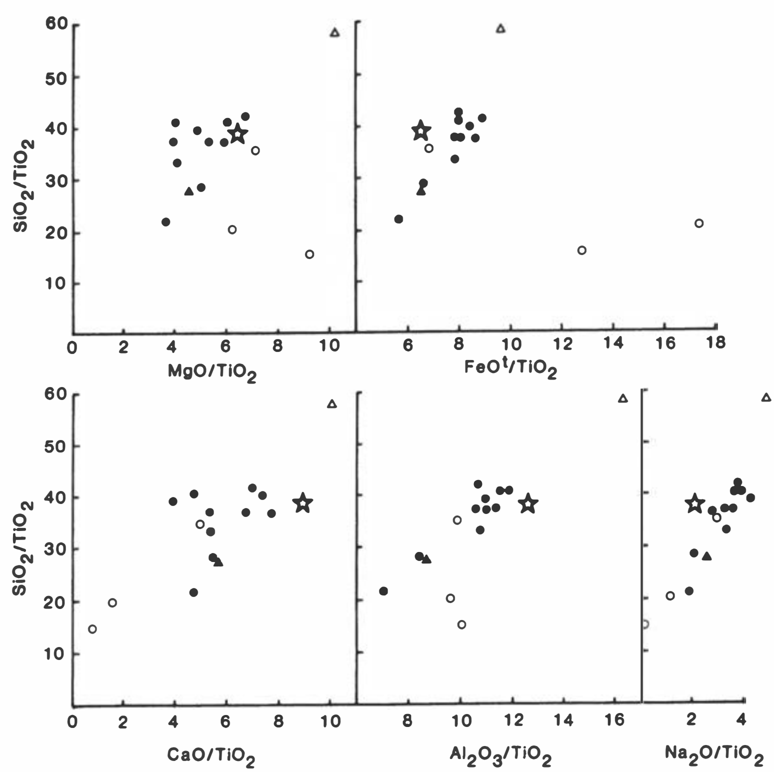


*Fig. 12.* Ratio variation diagrams showing compositional variations between host greenstones (closed symbols) and hydrothermally altered footwall rocks (open symbols) at Dragset. Circles are metabasalts, triangles metadolerites, star typical mid-ocean ridge basalt (Schilling et al. 1983).

some depletion in $SiO_2$ relative to $Al_2O_3$ and MgO in the stringer zone. Some depletion in CaO and $Na_2O$ is also suggested.

# Discussion

## *Ore-forming processes*

A number of features at the Dragset deposit indicate that the ores were initially formed by fluid circulation through oceanic-type crust and exhalative deposition soon after this crust was formed. The deposit contains two distinct ore types which could correspond to a fine-grained, massive component deposited on the sea floor as a sulphidic mound or sheet; and a feeder for the exhaled fluids, represented by a stringer zone showing epigenetic characteristics (cf. Rona 1984). The stringer zone shows enclosing hydrothermal alteration, and independent facing evidence indicates that it lies within the stratigraphic footwall. It is conceivable that the massive sulphide layers were also deposited beneath the sea floor by precipitation from hydrothermal fluids moving along a permeable zone between basalt flows (i.e a leaky hydrothermal system (cf. Rona 1984)). While this could account for the numerous separate massive ore layers, the field evidence does not generally support this model. The host basalts appear to have been very tight sheet flows with no significant interlayered permeable zones such as thick hyaloclastite beds. Individual layers of massive ore are always very sulphide-rich and do not contain major host rock inclusions. The presence of some layer-conformable siliceous and chloritic bands within the massive ores is also more consistent with deposition of mixed sulphide and non-sulphide exhalites on the sea floor. Finally, there are alternative explanations for the presence of multiple ore layers (see below). Ore deposition must have occurred at an early stage in the history of the greenstones, since dolerite dykes, probably related to ocean crust forming processes, have been intruded into the stringer zone and some massive ore layers. One of these dykes within the stringer or feeder zone also shows hydrothermal alteration (silicification and chloritization (Fig. 12)), suggesting that fluid circulation continued after dyke emplacement. Overturning of the orebody, recumbent folding and later upright folding of the disrupted massive sulphide lens(es) indicates that the mineralization predates all the recognizable deformation in the enclosing rocks, consistent with a syngenetic origin.

The stacked nature of the separate massive ore layers requires explanation. In some cases superimposed layers are clearly the same lens which has been recumbently folded upon itself or broken up by imbricate shearing (e.g. Fig. 9). It is not possible, however, to show that the whole orebody is a disrupted single layer. Conceivably there could have been several overlapping massive ore lenses fed from different feeders in the general area, although nowhere is it possible to see feeder structures cutting earlier massive sulphide layers. Given the degree of structural disruption within the ore horizon, the most that can be said about the original geometry of the orebody is that it consisted of one or a number of massive sulphide lenses overlying a well developed feeder zone. These were subsequently fragmented into a larger number of layers during the regional deformation.

A feature of the Dragset deposit which sets it apart from other documented deposits in the Løkken area is the abundance of pyrrhotite in the ores, particularly in the stringer ores. This pyrrhotite appears to be primary in origin as there is no textural evidence to suggest significant breakdown of pyrite to pyrrhotite during metamorphism; the abundance of pyrrhotite also varies greatly in different parts of the deposit and is independent of the pyrite content. Deposition of primary pyrrhotite would indicate highly reduced fluid conditions, particularly in the subsurface feeder. The lesser abundance of pyrrhotite in the pyritic massive ores and presence of magnetite with sphalerite in some sections is consistent with less reducing conditions during deposition on the sea floor.

Ore fabrics in Zn-rich ores suggest that these formed by replacement processes, after introduction of Zn into pre-existing pyritic ore, possibly via cooler and more oxidized fluids. The more oxidized mineral assemblage in these ores and their development in peripheral parts of the deposit might indicate greater interaction of oxidized seawater with hydrothermal fluid as a mechanism for major sphalerite precipitation (cf. Large 1977).

## *Ore deformation and recrystallization*

Macroscopic observation of the massive ore layers, particularly around $F_1$ folds, indicates that they have deformed in a semi-ductile manner, initially forming folds which then fragmented by brittle fracture in the tightening hinge zones. This break up, together with imbrication along the axial surface direction, produced a series of separate ore masses which mainly represent the dismembered limbs of isoclinal folds. As a result of this type of deformation fold hinges are not commonly preserved and it can be difficult to recognize the folds.

In highly pyritic ores, macroscopic ductility can be achieved at low temperatures (<450°C) through cataclastic flow and solution transfer (e.g. McClay & Ellis 1983, 1984; Cox 1987; Marshall & Gilligan 1987). The presence of significant intergranular chalcopyrite, which at the same temperatures readily deforms by dislocation mechanisms, would enhance this ductility. At Dragset, pyritic ore adjacent to late-stage faults preserves evidence of cataclastic flow which has resulted in a new ore fabric (Fig. 10D). Cataclasis appears to have involved brittle fracture, granulation, intragranular microfracture extension and rotation of grains to produce aligned granular aggregates of fractured pyrite. Similar textures could have developed during earlier recumbent folding and axial plane shearing of the massive ore layers given that PT conditions were favourable for brittle behaviour of pyrite. Many of the massive pyrite-rich ores exhibit what is essentially a recrystallized granulated fabric in which pyrite aggregates show a preferred orientation of their elongation (Fig. 10E, F). Structural etching reveals mostly equant grains and some non-aligned subgrain structures within these aggregates, suggesting recrystallization annealing and strain relief by subgrain growth. These features could be explained by earlier cataclastic deformation and flow of pyrite followed or accompanied by recrystallization. Textures indicating brittle fracture of large pyrite grains, together with infilling of extension microfractures with chalcopyrite, sphalerite and quartz are also consistent with cataclastic deformation of pyrite and mechanical or solution transfer of material into fractures. Chalcopyrite pressure shadows around some pyrite subhedra in chloritic layers further attest to rigid behaviour of pyrite in contrast to chalcopyrite (Fig. 10C).

## *Regional implications*

The primary tectonic settings of the various greenstone sequences in the Trondheim region are not yet fully resolved. The whole volcano-sedimentary sequence containing the Løkken greenstones has been interpreted by Roberts et al. (1984) as having formed in a marginal basin with various ophiolite fragments in the western Trondheim area representing phases of extensive crustal thinning and oceanic crust development within the basin (see also Grenne 1988). Geochemical data from the Løkken greenstones, including the data presented here, are consistent with an ocean-floor setting. The marked lack of terriginous sediment in the Løkken greenstones suggests a sediment-starved oceanic spreading centre at this stage of development. The presence of at least two distinct greenstone sequences (upper and lower metavolcanites, cf. Grenne et al. 1980) raises important questions about the tectonic setting. Possible explanations for this include reactivation or development of a new volcanic spreading centre in an area of existing oceanic crust represented by the lower greenstones.

Comparison of the greenstones in the Dragset area with those further east around Løkken indicates that the Dragset deposit and the small nearby Åsskjerp deposit (Fig. 2) occur at a lower stratigraphic level than the Løkken or Høidal deposits. The latter lie on the same horizon within the upper metavolcanic sequence, close to the lower contact of this subgroup with the lower metavolcanites (Grenne et al. 1980). This interpretation means that the Dragset and Åsskjerp occurrences comprise another mineralized level, and that the lower greenstones are prospective for other massive sulphide deposits. These small, lower deposits may in fact represent precursors to major sulphide deposition at a more favourable hiatus in volcanism, now represented by the large Løkken deposit.

Observations of metabasalts and gabbros in the lower greenstones away from sulphide deposits indicate that trace disseminated sulphides, mainly pyrite, chalcopyrite and pyrrhotite, are widespread in these rocks, both in the groundmass and as inclusions in silicate minerals. Unpublished company data (G. Grammeltvedt, pers. comm. 1985) also indicate that the lower parts of the greenstone succession show the highest background S contents and a stronger correlation between Cu, Zn and S than the upper greenstones. While it is likely that some of these trace sulphides were introduced by hydrothermal processes (Heim et al. 1986) it is also possible that some represent relicts of an immiscible sulphide phase developed in the original lavas during their emplacement and cooling. Such primary sulphides would be a good source of metal and S for later leaching by circulating seawater convection cells (cf. Strong & Saunders 1988; Kawahata & Shikazono 1988), particularly as the metals would be more readily stripped from these sulphides than from silicate minerals (Keays 1987).

Compositionally, the ores at Dragset are very similar to those at the major Løkken deposit (Astrup section, Table 2). The mean Cu/Zn ratio is similar, and the average total contents of Cu and Zn are approximately the same for the two deposits, with Dragset perhaps being slightly more Zn-rich. The Pb and Co values at Dragset appear to be lower than those at Løkken. The Høidal ores are somewhat more Zn-rich with lower Cu and higher Pb, Ag and Cd. These chemical similarities, together with the highly pyritic nature of the ores and other common features suggest a broadly similar mode of formation for all three deposits. The very low Pb content of all the deposits is consistent with the composition of the host metabasalts (<10 ppm Pb) and the general lack of pelitic sediments or felsic volcanics in the lower greenstone sequence, if this sequence is invoked as a metal source. This contrasts with some other volcanogenic deposits in central Norway (e.g. Killingdal and others in the Røros area) which have higher Pb contents in the ores but also a significant component of pelitic sediments in the volcano-sedimentary sequence.

Regional deformation of the Løkken area involved emplacement of the greenstone sequence (Støren Nappe) as part of the Trondheim Nappe Complex, probably by overthrusting (Oftedahl 1980). Several periods of folding, possibly before and certainly during and after nappe transport, produced the present configuration of folded nappe layers (e.g. Wolff & Roberts 1980). Structures at Dragset and in the surrounding area are consistent with two main phases of folding, followed by a third deformation. Early, large-scale, recumbent isoclinal folding ($F_1$) was followed by open upright folding ($F_2$) which deformed the stratigraphic layering (including the ore layers) and $S_1$ surface, and produced the asymmetric Løkken synform. A steep, south dipping axial surface ($S_2$) was variably developed during this folding, showing its strongest expression in the steep, highly strained northern limb of the synform. Progressive increase in strain across the synform thus accounts for the zone of greenschists along its northern side (Fig. 13). Major thrusts appear to have been initiated during or soon after the $F_2$ folding, as they have not been folded by the major $F_2$ synform. Thrusting may have been in response to compressive stresses related to irregular shortening and space constraints within the core of the Løkken synform. The thrust faults also acted as the locus for further movement during later deformation. High-angle faults appear to have formed during east–west compression along the axis of the Løkken synform after the $F_2$ folding. This late deformation may also account for the plunge reversals along the main synformal axis and minor kink folding and crenulation of $S_2$. Smaller faults and fractures probably include early structures related to the larger cross-cutting high-angle faults as well as some faults, including normal faults, related to post-compressional stress relief within the synform. Studies in other parts of the Trondheim Nappe Complex (e.g. Olesen et al. 1973; Guézou 1978; Rickard 1985) suggest an earlier deformation, not evident at

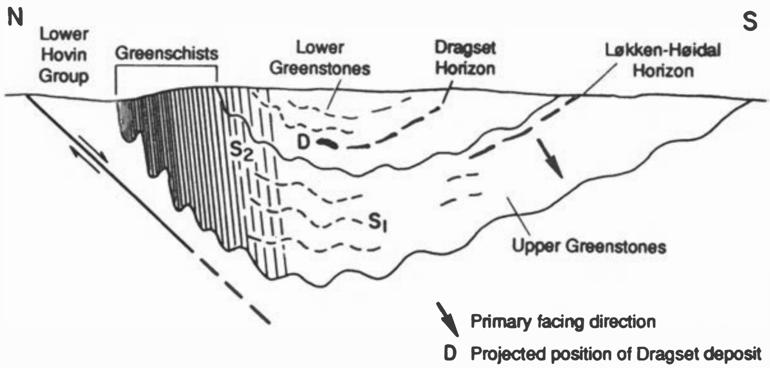


*Fig. 13.* Diagrammatic cross section of the Løkken Synform showing the main structural elements, variation in strain across the structure and the relative stratigraphic positions of the Løkken–Høidal and Dragset mineralized horizons.

Dragset, so that the $F_1$ and $F_2$ folding events described here possibly equate with regional $F_2$ and $F_3$ phases of folding.

The regional deformation has clearly modified the Dragset ores but most also have affected the other deposits in the Løkken synform. There is little documentation of deformation features at the major Løkken deposit but some cursory observations revealed a number of structures consistent with the type of deformation obvious at Dragset. Generally the thick massive ore lenses at Løkken show no clear evidence of major tectonic folding. However, where the ore layers are thinner, for example in a small lens intersected by a decline on the lowest level of the mine, fold structures very similar to those at Dragset can be seen. At this locality the massive ore lens has been recumbently folded into a large-scale isoclinal fold with a low plunge to the north (Fig. 14B, C). The sulphide layer shows disruption by brittle fracture in the hinge zone and there is also a high angle reverse fault across the hinge. Similar fold structures occur further down the decline and these have low angle plunges to the north and northwest. Some small upright folds also occur in this area and possibly correspond to the $F_2$ generation of folds at Dragset. Copper and Zn distributions in very thick parts of the main orebody may also reflect folding of the ore (Fig. 14A; R. Juhava, pers. comm.) and in some areas thrust structures appear to control the configuration of the ore masses. These observations at least indicate that the Løkken deposit has suffered the regional deformation history and has probably been modified by this deformation to a greater extent than previously realized.

## Conclusions

The Dragset Cu–Zn deposit consists of stratabound massive sulphides and a well-defined footwall stringer zone. The deposit probably formed by sulphide deposition from cooling hydrothermal fluids circulating through and discharging into ocean-floor crust soon after this crust was formed. The focused ore fluids caused localized hydrothermal alteration around the stringer zone. This resulted in enrichment in MgO and FeO, together with depletion in $Na_2O$ and CaO, in the inner parts and some silicification in the outer parts. In terms of modern analogues, the general characteristics of the deposit and enclosing host rocks, particularly the dominance of sheet flows, lack of pelagic sediments or major siliceous exhalites, high pyrrhotite content, presence of high-Fe sphalerite and absence of barite, suggest an immature type of ocean-floor deposit probably formed by actively venting, high temperature fluids (cf. Hannington et al. 1986, 1989).

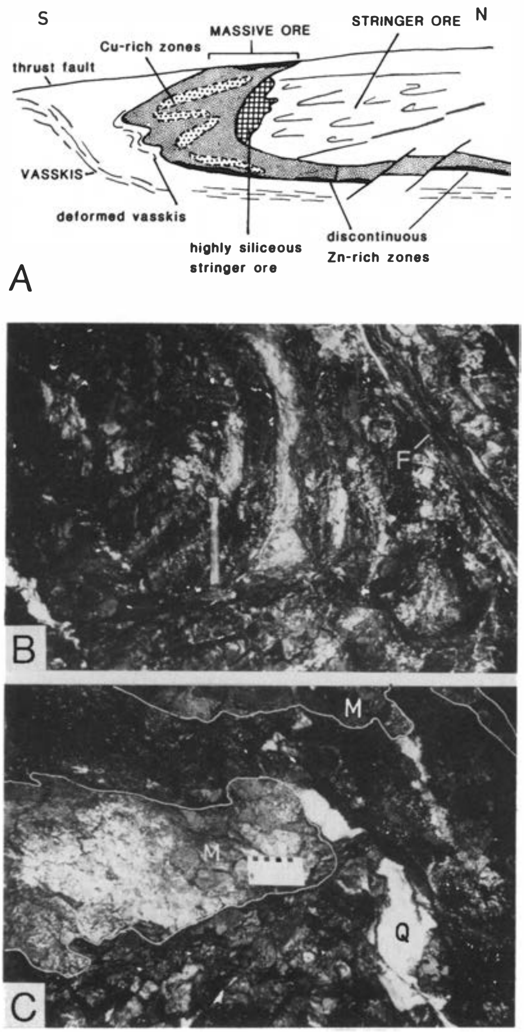


*Fig. 14.* Mesoscopic ore structures at the Løkken deposit illustrating deformation similar to that at Dragset. A. Diagrammatic cross section through the western part of the Løkken orebody, Astrup section. B. Hinge zone of recumbent fold affecting massive ore and the enclosing greenstone and vasskis rocks, seen in ramp at decline level (S.S. 151) Astrup section. Note also small reverse fault at right. View looking ENE. C. Detail showing folded and fragmented massive sulphide lens (M) in hinge zone of recumbent fold. Note also dilational quartz vein (Q). Black and white scale is in cm.

Location of the Dragset deposit at a lower stratigraphic level than the Løkken and Høidal deposits indicates that ore-forming processes operated at more than one time in the history of the Løkken greenstones. However, all significant mineralization appears to be within or immediately above the lower greenstone sequence.

After deposition, the Dragset deposit was strongly deformed by at least two major folding events. Peak metamorphism appears to have predated the second stage of folding. Early deformation resulted in isoclinal, recumbent folding of the massive ore layers and accompanying segmentation by axial plane shearing. The feeder zone was also flattened and extended parallel to the major fold axis direction. Later upright folding accompanied development of the Løkken synform and produced open to tight mesoscopic folds of the massive ore layers and a variably developed axial surface in the feeder zone and host rocks. The Dragset ores illustrate well the style of deformation which is probably common in massive pyritic ores subjected to high shear stress under low grade metamorphic conditions (350–450°C). Brittle-ductile deformation of fine-grained, highly pyritic ore probably occurred largely by cataclastic flow involving granulation and grain boundary sliding. Such behaviour allowed folding of massive ore layers before disruption by failure of the hinge zones to produce a closely spaced stack of separate or partly connected sulphide lenses. Evidence for similar deformation can be seen on a mesoscale in the western part of the major Løkken deposit. The ores at Løkken also show the same type of deformation and annealing recrystallization textures to those at Dragset. The smaller Høidal deposit west of Løkken appears to be less deformed and preserves more relict primary textures such as colloform pyrite and sphalerite (cf. Grenne & Vokes 1986).

*Acknowledgements.* – This study was undertaken as part of a study leave programme at the Geologisk Institutt, NTH, Universitetet i Trondheim. Financial and logistic support was received from the Geologisk Institutt, Løkken Gruber A/S, Norges geologiske undersøkelse and the Canberra College of Advanced Education. I sincerely thank F. M. Vokes, G. Juve and G. Grammeltvedt for organizing the project and for their encouragement and discussions at various stages of the work. T. Grenne and R. Juhava introduced me to the greenstones and ores of the Løkken area. I also thank Kjetil Mjøen for assistance in the field. Technical support was provided by I. Rømme, A. Monsøy, K. Isachsen and L. Skjellum at the Geologisk Institutt and L. Wensing, F. Krikowa and R. Mason at the CCAE. The original manuscript was improved by the constructive comments of F. M. Vokes, T. Grenne and the two reviewers, N. Odling and O. Nilsen.

Manuscript received April 1989

# References

Borchgrevink, O. F. 1954: Teknisk utvikling ved Gruben. In *Løkken Verk En Norsk Grube: Gjennom 300 Ar*, 505 pp. F. Bruns Bokhandels Forlag, Trondheim.

Carstens, C. W. 1951: Løkkenfeltets geologi. *Norsk Geologisk Tidsskrift 29*, 9–25.

Cox, S. F. 1987: Flow mechanisms in sulphide minerals. *Ore Geology Reviews 2*, 133–171.

Grenne, T. 1986: Ophiolite-hosted Cu–Zn deposits at Løkken and Høydal, Trondheim Nappe complex, upper allochthon. *In* Stephens, M. B. (ed.): *Stratabound Sulphide Deposits in the Central Scandinavian Caledonides: Excursion Guide No. 2, 7th IAGOD Symposium, Uppsala, 1986: Sveriges Geologiska Undersokning 60*, 55–68.

Grenne, T. 1988: Marginal basin type metavolcanites of the Hersjø Formation, eastern Trondheim District, Central Norwegian Caledonides. *Norges geologiske undersøkelse 412*, 29–42.

Grenne, T., Grammeltvedt, G. & Vokes, F. M. 1980: Cyprus-type deposits in the Western Trondheim district, central Norwegian Caledonides. *In* Panayiotou, A. (ed.): *Ophiolites: Proceedings of the International Ophiolite Symposium, Cyprus, 1979, Nicosia: Cyprus Ministry Agriculture Natural Resources, Geol. Survey Dept.*, 727–743.

Grenne, T. & Vokes, F. M. 1986: Sea-floor sulphide paragenesis at the Høydal stratabound sulphide ore, Central Norwegian Caledonides. Abstract: *Terra Cognita, 7th quadrennial IAGOD symposium, Luleå, 1986*, p. 502.

Guézou, J. C. 1978: Geology and structure of the Dombås–Lesja area, Southern Trondheim Region, South-central Norway. *Norges geologiske undersøkelse 340*, 1–34.

Hannington, M. D., Peter, J. M. & Scott, S. D. 1986: Gold in seafloor polymetallic sulfide deposits. *Economic Geology 81*, 1867–1883.

Hannington, M. D., Scott, S. D. & Herzig, P. M. 1989: Geochemical controls of gold mineralization in massive sulfide deposits of modern ocean floor and their ancient analogs. *28th International Geological Congress, Washington, D.C.* 1989, *Abstracts* 2, 2–24.

Harris, D. C., Cabri, L. J. & Nobiling, R. 1984: Silver-bearing chalcopyrite, a principal source of silver in the Izok Lake massive-sulfide deposit: confirmation by electron- and proton-microprobe analyses. *Canadian Mineralogist 22*, 497–502.

Heim, M., Grenne, T. & Prestvik, T. 1986: The Resfjell ophiolite fragment, southwest Trondheim region, Central Norwegian Caledonides. *Norges geologiske undersøkelse 409*, 49–72.

Kawahata, H. & Shikazono, N. 1988: Sulfur isotope and total sulfur studies of basalts and greenstones from DSDP hole 504B Costa Rica Rift: implications for hydrothermal alteration. *Canadian Mineralogist 26*, 555–565.

Keays, R. R. 1987: Principles of mobilization (dissolution) of metals in mafic and ultramafic rocks – The role of immiscible magmatic sulphides in the generation of hydrothermal gold and volcanogenic massive sulphide deposits. *Ore Geology Reviews 2*, 47–63.

Large, R. R. 1977: Chemical evolution and zonation of massive sulfide deposits in volcanic terrains. *Economic Geology 72*, 549–572.

Marshall, B. & Gilligan, L. B. 1987: An introduction to remobilisation. Information from ore-body geometry and experimental considerations. *Ore Geology Reviews 2*, 87–131.

McClay, K. R. & Ellis, P. G. 1983: Deformation and recrystallization of pyrite. *Mineralogical Magazine 47*, 527–538.

Nicholls, J. 1988: The statistics of Pearce element diagrams and the Chayes closure problem. *Contributions to Mineralogy and Petrology 99*, 11–24.

Oftedahl, Chr. 1980: Geology of Norway. *Norges geologiske undersøkelse 356*, 3–114.

Olesen, N. Ø., Hansen, E. S., Kristensen, L. H. & Thyrsted, T. 1973: A preliminary account on the geology of the Selbu–Tydal area, the Trondheim region, Central Norwegian Caledonides. *Leitse 49*, 259–276.

Pearce, T. H. 1968: A contribution to the theory of variation diagrams. *Contributions to Mineralogy and Petrology 19*, 142–157.

Pearce, J. A. 1975: Basalt geochemistry used to investigate past tectonic environments on Cyprus. *Tectonophysics 25*, 41–67.

Pearce, J. A. & Cann, J. R. 1973: Tectonic setting of the mafic volcanic rocks determined using trace element analyses. *Earth and Planetary Science Letters 19*, 290–300.

Rickard, M. J. 1985: The Surnadal Synform and basement gneisses in the Surnadal–Sunndal district of Norway. *In* Gee, D. G. & Sturt, B. A. (eds.): *The Caledonide Orogen – Scandinavia and Related Areas*, 485–497. Wiley, New York.

Roberts, D., Grenne, T. & Ryan, P. D. 1984: Ordovician marginal basin development in the central Norwegian Caledonides. *In* Kokelaar, B. P. & Howels, M. F. (eds.): *Marginal Basin Geology: Geological Society of London, Spec. Publ. 16*, 233–244.

Rona, P. A. 1984: Hydrothermal mineralization at seafloor spreading centers. *Earth Science Reviews 20*, 1–104.

Ryan, P. D., Skevington, D. & Williams, D. M. 1980: A revised interpretation of the Ordovician stratigraphy of Sør-Trøndelag and its implications for the evolution of the Scandinavian Caledonides. *In* Wones, D. R. (ed.): *The Caledonides in the U.S.A.: Virginia Polytechnic Inst. and State Univ. Dept. Geol. Sci. Memoir 2*, 99–103.

Sangster, D. F. 1972: Precambrian volcanogenic massive sulphide deposits in Canada: a review. *Canadian Geological Survey Pap. 72–22*, 43 pp.

Schilling, J. G., Zajac, M., Evans, R., Johnston, T., White, W., Devine, J. D. & Kingsley, R. 1983: Petrologic and geochemical variations along the mid-Atlantic Ridge from 27°N to 73°N. *American Journal of Science 283*, 510–586.

Solomon, M. & Walshe, J. L. 1979: The formation of massive sulfide deposits on the sea floor. *Economic Geology 74*, 797–813.

Strong, D. P. & Saunders, C. M. 1988: Ophiolitic sulphide mineralization at Tilt Cove, Newfoundland: Controls by upper mantle and crustal processes. *Economic Geology 83*, 239–255.

Vokes, F. M. 1960: Løkken pyrite mine. *In* Vokes, F. M. (ed.): *Mines in South and Central Norway, Excursion Guide C10 21st International Geological Congress, Oslo*, 64–73.

Winkler, H. G. F. 1979: *Petrogenesis of Metamorphic Rocks.* 5th ed. 348 pp., Springer Verlag, New York.

Wolff, F. Chr. 1976: Geologisk kart over Norge, berggrunnskart Trondheim 1:250,000. Norges geologiske undersøkelse, Trondheim.

Wolff, F. Chr. & Roberts, D. 1980: Geology of the Trondheim region. *Norges geologiske undersøkelse 356*, 117–128.